

High-resolution Zeeman spectroscopy of Ni^{2+} in ZnS

R. Heitz, A. Hoffmann, and I. Broser

Institut fuer Festkoerperphysik, Technische Universitaet Berlin, Hardenbergstrasse 36, 10623 Berlin, Germany

(Received 13 May 1994)

In ZnS the ${}^3T_1(F)$ - ${}^3T_1(P)$ transition of isolated Ni^{2+} causes structured near infrared absorption and emission bands. Crystals doped in the sub-ppm region exhibit exceptionally sharp lines suited to study the dependence on external fields. Here, the fine structure of the perfectly cubic and one axial Ni^{2+} center is studied. A secure assignment of the observed optical transitions is achieved on the basis of high-resolution absorption and emission investigations at various crystal temperatures and in magnetic fields up to 15 T. The experimental results give evidence for intermediate dynamical Jahn-Teller effects in both the ${}^3T_1(F)$ ground and the ${}^3T_1(P)$ excited state, which are attributed to the coupling to local T_2 -type modes. A detailed comparison shows good agreement between the experimental data for ZnS:Ni and those of the well understood system CdS:Ni. A Fano-type structure in the ${}^3T_1(F)$ - ${}^3T_1(P)$ absorption is explained by the coupling of a distinct local mode of the Ni center to a continuum of phonon states. Additionally, the interaction of low-frequency acoustical phonons with the Ni center is investigated. No thermal equilibrium is established in the excited ${}^3T_1(P)$ state during its lifetime, which gives rise to hot emission lines.

I. INTRODUCTION

Energy levels of transition metal ions incorporated in semiconductors are strongly influenced by the surrounding lattice. Transitions between such energy levels result in sharp lines as well as broad bands in absorption and emission yielding information on the static crystal field, the covalent bonding, and interactions with lattice vibrations. In general, the analysis of the spectra is difficult; only the observed fine structure and its dependence on external fields allows the unambiguous assignment of the spectral lines in a theoretically developed energy scheme. Especially for Jahn-Teller active systems the experimental determination of the irreducible representations of the involved energy levels is essential. Thus, thorough experimental data are necessary to develop and prove theoretical concepts in order to get detailed insight into the basic interactions determining the electronic or vibronic structure of transition metal centers.

The incorporation of nickel ions on cation sites in the wideband gap II-VI semiconductors leads to a variety of absorption^{1,2} and emission³ bands due to intracenter transitions between crystal field states. The fine structure of the crystal field states of Ni^{2+} in ZnS was first investigated by Weakliem² and discussed considering spin-orbit interaction. Subsequently, much work has been devoted to the study of Ni^{2+} in ZnS. The increasing quality of the investigated samples enabled high-resolution investigations of the fine structure,⁴⁻⁸ of the excitation behavior,^{9,10} as well as of influences of magnetic fields,¹¹⁻¹³ of pressure,^{14,15} and of the Ni mass.¹³ Recently, the observation of exceptionally fast relaxation processes for Ni^{2+} centers in ZnS initiated a series of investigations¹⁶⁻¹⁹ concerning the radiative and nonradiative relaxation channels in this multilevel system. All investigations gave hints for an electron-phonon coupling, but only few attempts^{4,5} to calculate these cou-

plings have been made yet. The reason is the difficulties with the identification of the fine structure of the cubic Ni^{2+} center resulting from the polymorphic crystal structure of ZnS. Additionally, the confusing appearance of the M band in the spectral region of the ${}^3T_1(P)$ - ${}^3T_1(F)$ luminescence^{12,13} could be resolved only recently.²⁰

On the basis of thorough experimental data^{13,21} for the ${}^3T_1(F)$ - ${}^3T_1(P)$ transition of Ni^{2+} in CdS a detailed description²²⁻²⁴ of the fine structure considering simultaneously the spin-orbit interaction, the trigonal crystal field, and the Jahn-Teller coupling has been developed. It is demonstrated that by fitting the observed optical transitions, both the Zeeman behavior and isotope shifts are reproduced too, demonstrating a fundamental understanding of the fine structure interactions. The experimental data of the system CdS:Ni are explained by an intermediate Jahn-Teller coupling to high-energy T_2 -type local modes in both the ${}^3T_1(F)$ and the ${}^3T_1(P)$ state. On the contrary, the fine structure of the ${}^3T_1(P)$ state of Ni^{2+} in ZnS has been explained by an intermediate coupling to two acoustical phonons having E and T_2 symmetry.⁵ However, only the four lowest absorption lines have been considered. In view of the similar environment of Ni on cation sites in ZnS and CdS, the electron phonon interaction should be rather similar in both systems, initiating a reinvestigation of the system ZnS:Ni. A secure assignment of the fine structure to specific Ni centers as well as high-resolution data would allow us to check the theoretical approach explaining successfully the corresponding data in CdS:Ni.

In the present work the fine structure of the ${}^3T_1(F)$ - ${}^3T_1(P)$ transition of isolated Ni^{2+} ions in ZnS is investigated by means of high-resolution absorption and emission spectroscopy. The aim is to gain thorough data giving a hard fundament for theoretical considerations. Therefore, the fine structure of the cubic Ni^{2+} center is investigated in dependence on magnetic fields and crys-

tal temperature, allowing a clear identification of the observed transitions. The fine structure of the ${}^3T_1(F)$ ground as well as the ${}^3T_1(P)$ excited state is discussed in the framework of a dynamical model, demonstrating intermediate Jahn-Teller effects in both states. A detailed comparison with the system CdS:Ni yields a qualitative understanding of the fine structure interactions.

II. EXPERIMENT

For the spectroscopic investigations the samples were immersed in superfluid He or mounted in a continuous He gas flow of variable temperature. Absorption measurements were performed in a polychromatic arrangement using a tungsten lamp, a 0.75 m double-grated monochromator (Spex Industries), and a cooled GaAs photomultiplier. The luminescence was excited either by the 476 nm line of an Ar^+ laser (Spectra Physics) or at 652 nm using a dye laser system (Coherent). For the Zeeman experiments a 15 T superconducting magnet built in split-coil configuration (Intermagnetics and Janis, Inc.) was used.

The investigated ZnS crystals were high-quality bulk specimens with dimensions in the millimeter range grown by R. Broser using the Frerichs-Warminski method.²⁵ In principle, these crystals have a polymorphic crystal structure, but the investigated samples were selected for their nearly perfect cubic appearance. The samples were doped with nickel in the sub-ppm region by evaporating a controlled Ni layer onto the crystal surfaces and a subsequent annealing at temperature around 800 °C for 2–48 h. A more detailed description of the growth and doping procedure is given elsewhere.¹³ The crystals contain Fe and Cu as residual impurities and have been used to study the respective intracenter transitions.^{26,27}

III. EXPERIMENTAL RESULTS

A. The ${}^3T_1(F)$ - ${}^3T_1(P)$ absorption

ZnS crystals doped with nickel in the ppm region exhibit a strong absorption band in the near infrared spec-

tral region (Fig. 1), which has been attributed to the ${}^3T_1(F)$ - ${}^3T_1(P)$ transition of isolated Ni^{2+} ions on Zn sites.² The absorption shows, on the high-energy side of the dominating zero phonon line (ZPL) O at 1.541 29 eV, a richly structured sideband. Kaufmann and Koidl⁵ claimed that the whole sideband, except for the first broad maximum shifted by 6.3 meV, can be assigned to "simple, unshifted phonon" replicas of the ZPL O corresponding to modes of the host lattice at critical points of the Brillouin zone. However, a distinct replica due to optical phonons or local modes would be expected in this case.^{20,26} The absence of these structures is rather a hint for a dynamical Jahn-Teller interaction in the excited ${}^3T_1(P)$ state and thus favors an interpretation in terms of vibronic states. In general, a moderate or strong Jahn-Teller interaction in the terminating state of an optical transition seems to suppress the appearance of clearly resolved host phonon replicas in the sideband.

Noteworthy is the sharp drop in the absorption at 1.5818 eV, shown enlarged in Fig. 2. Such resonances can result from the coupling of a discrete state with a continuum of states as proposed by Fano.²⁸ A Fano resonance occurring in a phonon sideband indicates an anharmonic coupling between a local mode of the impurity center and the continuum of host modes,²⁹ where the coupling of the phonon modes results from a Jahn-Teller effect in the terminating state. Thus the Fano resonance observed in the sideband of the ${}^3T_1(F)$ - ${}^3T_1(P)$ absorption (Fig. 2) indicates a dynamical Jahn-Teller effect in the excited ${}^3T_1(P)$ state and proves the vibronic character of the sideband. The line shape $f(\omega)$ of a Fano-type resonance is described by²⁸

$$f(\omega) = \frac{q^2 + 2\xi q - 1}{1 + \xi^2} \quad \text{with} \quad \xi = \frac{\hbar\omega - E_0}{\hbar\gamma}. \quad (1)$$

The parameter q depends on the interaction between the discrete state and the continuum of states as well as the relative oscillator strengths of the transitions into these states. $\hbar\gamma$ describes the damping of the discrete state and E_0 corresponds to the energy of the discrete state, but can deviate slightly from the energy this state

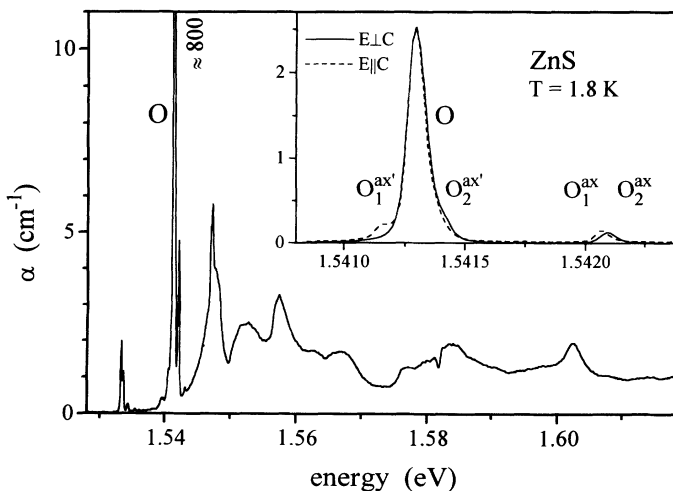


FIG. 1. The ${}^3T_1(F)$ - ${}^3T_1(P)$ absorption of Ni^{2+} observed for a nearly cubic ZnS crystal doped with about 0.5 ppm Ni at $T = 1.8$ K. The inset gives, on an enlarged energy scale, polarized spectra of the zero phonon region for an unintentionally doped sample. The polarized lines are attributed to axial centers.

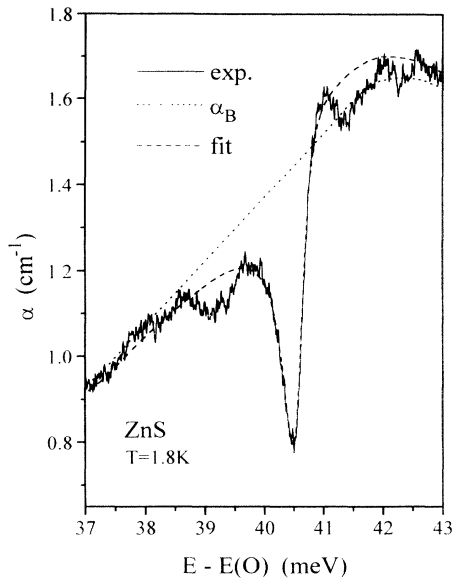


FIG. 2. Fano-type resonance in the sideband of the ${}^3T_1(F)$ - ${}^3T_1(P)$ absorption of Ni^{2+} in cubic ZnS at $T = 1.8$ K [$E(O) = 1.54129$ eV]. The experimental data, the theoretical fit, and the estimated background absorption (α_B) are given by full, dashed, and dotted lines, respectively. The parameters of the fit are given in the text.

would have without coupling.

The absorption coefficient α is given by

$$\alpha(\omega) = \alpha_B(\omega)[1 + pf(\omega)]. \quad (2)$$

$\alpha_B(\omega)$ describes the broad background absorption due to the continuum of states and p takes into account that only part of these states contributes to the coupling. The dashed line in Fig. 2 represents a fit with $E_0 = 40.55$ meV, $\hbar\gamma = 0.21$ meV, $q=0.33$, and $p = 0.45$, reproducing reasonably well the experimental spectrum. The discrete phonon mode with an energy of 40.55 meV lies in the gap between the transversal and longitudinal optical phonons and thus is a local gap mode. The observed damping corresponds to a lifetime of 3.1 ps of this mode. It should be noted that we observe similar resonances for the ${}^3T_1(F)$ - ${}^3T_1(P)$ absorption of Ni^{2+} in CdS shifted by 17.0 and 17.6 meV with respect to the $O_{1,2}$ doublet.

In the spectral region of the ZPL O a lot of additional fine structure is resolved in Fig. 1. These lines are a consequence of the polymorphic crystal structure¹³ as well as the formation of Ni pairs.⁶ Up to now both processes have prevented the secure assignment of the fine structure and therefore a detailed investigation of the cubic Ni^{2+} center. The absorptions occurring around 1.534 and 1.548 eV are polarized and their intensity with respect to that of the cubic ZPL O varies drastically with the investigated sample. They are attributed to Ni ions in different axial surroundings provided by the polymorphic crystal structure of ZnS. The weak resonances on the low-energy slope of the ZPL O are found to be unpolarized and could be resolved in crystals containing at least 0.5 ppm Ni only. Both observations are consistent with

an assignment to Ni pairs in spite of the low probability of statistical pair formation at concentrations around 0.5 ppm.³⁰

The inset of Fig. 1 depicts polarized high-resolution absorption spectra for an undoped ZnS sample having an increased number of axial crystal regions. The unpolarized ZPL O having a full width at half the maximum (FWHM) of 80 μeV clearly belongs to Ni in a perfectly cubic environment. Recently, a weak absorption resonance observed 800 μeV on the high-energy side of the ZPL O has been attributed to the cubic Ni^{2+} center too.^{5,11} Nevertheless, the weak absorption resonance shown in the inset at the same energy position consists of a strongly polarized doublet $O_{1,2}^{\text{ax}}$ with an energy splitting of 35 μeV and its relative intensity with respect to that of the cubic ZPL O depends on the investigated sample. No polarization is expected in cubic symmetry and thus this doublet cannot be assigned to the cubic Ni^{2+} center indicating an axial one. Similar considerations hold for the resonances $O_{1,2}^{\text{ax}'}$ at the onsets of the ZPL O .

In order to identify the fine structure of the excited ${}^3T_1(P)$ state of the cubic Ni^{2+} center we performed Zeeman experiments. Figure 3 gives the results of polarization-dependent high-resolution Zeeman measurements on a predominantly cubic ZnS sample for the magnetic field oriented parallel either to the $[110]$ axis or to the $[111]_{\text{gr}}$ growth direction. A complicated line pattern is observed in both orientations which represents directly the magnetic field dependence of the fine structure in the excited ${}^3T_1(P)$ state since the A_1 - ${}^3T_1(F)$ ground state is diamagnetic up to 15 T.²⁴ The dominating ZPL O of the cubic center splits into a triplet and the observed polarizations are found to be consistent with the components of a T_2 state in C_s and C_3 symmetry, re-

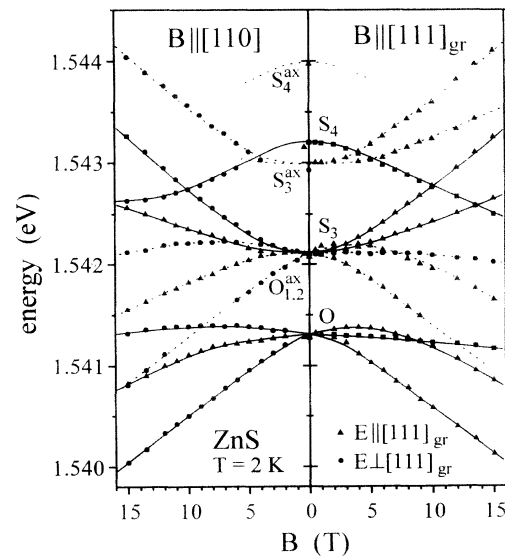


FIG. 3. The Zeeman behavior of the ZPL's of the Ni^{2+} [${}^3T_1(F)$ - ${}^3T_1(P)$] absorption of the cubic (full lines) and an axial (dotted lines) center in nearly cubic ZnS at $T = 2$ K observed in the Voigt configuration with the magnetic field aligned parallel to the $[110]$ and the $[111]_{\text{gr}}$ axis, respectively.

spectively. Remarkable is the level crossing occurring at $B = 8.5$ T in the configuration $B \parallel [111]_{\text{gr}}$. A similar behavior is observed in CdS at $B = 13.5$ T.¹³ Transitions into higher lying states not having T_2 character are forbidden in cubic symmetry and thus are not observed in zero field spectra. However, in a magnetic field transition from the A_1 ground state to all components of these states are allowed on principle. The magnetic field causes a mixing of the T_d wave functions leading to an increasing intensity of these transitions with increasing magnetic field strength. Indeed, at higher energies three components showing a strong increase in intensity with increasing field are observed and thus are attributed to the cubic center. These components exhibit strong non-linear shifts towards higher energies with increasing magnetic field demonstrating pronounced term interactions with the components of the cubic ZPL O . The components attributed to the cubic Ni^{2+} center are marked by full lines in Fig. 3. By extrapolating the zero field positions and exploiting the observed polarizations the Zeeman data yield an E and an A_1 state 830 and 1830 μeV above the T_2 state, respectively. The transitions from the $A_1-{}^3T_1(F)$ ground state into the T_2 , E , and A_1 components of the ${}^3T_1(P)$ state are labeled O , S_3 , and S_4 , respectively, corresponding to the nomenclature used for CdS:Ni .¹³

The remaining Zeeman components form a second set (marked by dotted lines in Fig. 3) shifted by 800 μeV towards higher energies indicating a further, nearly identical, Ni^{2+} center. Although the observed Zeeman pattern is nearly identical to that of the cubic center, no significant changes of the absorption strength of the components of the S_3^{ax} and the S_4^{ax} transitions are observed, indicating a lower symmetry of the center. Additionally, the $O_{1,2}^{\text{ax}}$ doublet corresponds exactly to the polarized doublet observed in zero field spectra (inset of Fig. 1) showing a trigonal splitting of 35 μeV . Thus we connect this axial center with the still polymorphic crystal structure of the investigated ZnS samples. The trigonal splitting of the T_2 state is very small compared to the fine structure and Zeeman splittings and thus does not sig-

nificantly alter the Zeeman behavior. By investigating crystals doped with enriched Ni isotopes we resolve an isotope splitting of 15 $\mu\text{eV}/\text{nucleon}$ for the axial $O_{1,2}^{\text{ax}}$, but none for the cubic O . Nevertheless, in view of the almost identical fine structure of both centers we attribute the missing isotope shift of the cubic center to the larger FWHM of its O line. The accidental degeneracy of the $O_{1,2}^{\text{ax}}$ transitions of the axial center and the S_3 transition of the cubic center confused the interpretation of the zero field spectra, but they are clearly distinguished in a magnetic field.

B. The ${}^3T_1(P)-{}^3T_1(F)$ luminescence

Figure 4 represents the ${}^3T_1(P)-{}^3T_1(F)$ luminescence observed for a Ni-doped ZnS crystal in reflection arrangement exciting in the blue spectral region via the $\text{Ni}^{2+}/+$ charge transfer transition.¹⁸ A weak emission at the exact position of the O absorption is followed by a dominating doublet E, E' around 1.5191 eV and a broad line E_4 at 1.4174 eV. The nomenclature is related to that introduced for the corresponding transitions in CdS .¹³ The threefold structure is typical for luminescence transitions ending in the ${}^3T_1(F)$ ground state of Ni^{2+} in the wideband gap II-VI semiconductors.^{8,13} These lines show weak and broad replica with energies corresponding to acoustical phonons, but no distinct replica due to optical host phonons. Instead, a series of six weak resonances shifted between 36.5 and 41 meV with respect to the ZPL O , as well as similar replica of the E, E' doublet, is observed. A corresponding phonon structure is resolved in the phonon sideband of the ${}^3T_1-{}^1T_1$ luminescence of W^{2+} in ZnS (Ref. 20) too, indicating a general process.

The ZPL O appears broad and weak in the luminescence of ZnS crystals doped with Ni in concentrations above about 0.1 ppm. The strong O absorption in connection with the omnipresent luminescence undergrowth suppresses the O emission due to self-absorption. On the contrary, unintentionally doped samples with neglectable absorption show the ZPL O with an intensity comparable

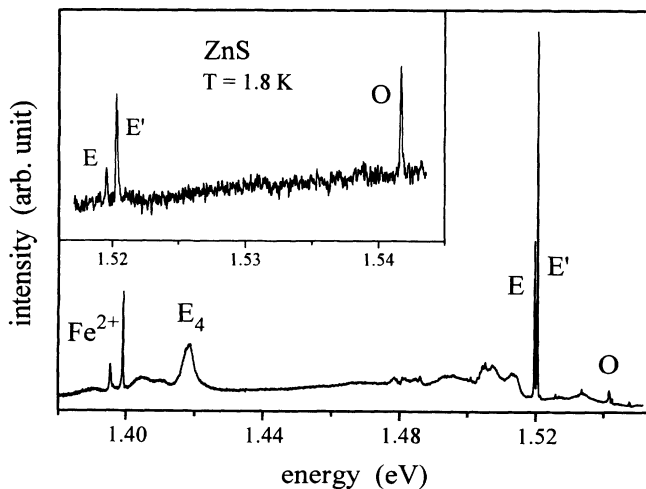


FIG. 4. The ${}^3T_1(P)-{}^3T_1(F)$ luminescence of Ni^{2+} observed for a nearly cubic ZnS sample doped with about 0.5 ppm Ni at $T = 1.8$ K excited at 2.605 eV. The two sharp lines around 1.398 eV result from the spin-forbidden ${}^3T_1(H)-{}^5E(D)$ transition of Fe^{2+} (Ref. 33). The inset shows the high energy region for an unintentionally doped sample.

to that of the E doublet (inset of Fig. 4). For such samples FWHM's of the O emission down to $100 \mu\text{eV}$ are observed, corresponding well to the $80 \mu\text{eV}$ measured for the O absorption of an undoped sample. Both the O absorption and emission seem to experience a strong increase of their FWHM's with increasing Ni concentration even for concentrations in the ppm region.¹³ In contrast, the FWHM's of the E emissions are not influenced by these Ni concentrations, indicating experimental difficulties resulting from the extraordinary high oscillator strength of this transition.¹⁸

The general structure of the ${}^3T_1(P)$ - ${}^3T_1(F)$ luminescence reflects the three spin-orbit components of the ${}^3T_1(F)$ ground state. However, the energy splittings are smaller than expected from static crystal field theory, indicating a Jahn-Teller interaction. Additionally, the doublet structure of the E lines cannot be explained in a static model, giving just one T_1 state in the corresponding energy region. Nevertheless, investigating a variety of different crystals the intensity ratio of the unpolarized E, E' doublet does not change. Both have to be connected with the cubic center. Figure 5 represents the temperature dependence of the E, E' doublet. Both lines become broader at temperatures above 5 K, but their intensity ratio is not altered. Thus the temperature-dependent measurements give no hint for thermalization effects, which would prove the splitting to originate in the excited ${}^3T_1(P)$ state. The integrated intensity decreases with increasing temperature and above 40 K no lines could be resolved any longer.

To evaluate the origin of the E, E' doublet we investigated its Zeeman behavior. Figure 6 shows the development of the E, E' doublet in a magnetic field oriented parallel to the $[110]$ axis and the polarization $E \perp B$. With increasing magnetic field the intensity of the com-

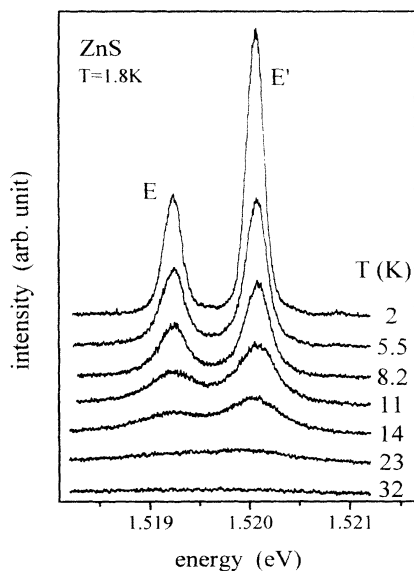


FIG. 5. The E, E' doublet of the ${}^3T_1(P)$ - ${}^3T_1(F)$ luminescence of Ni^{2+} in cubic ZnS at different crystal temperatures. The luminescence is excited resonantly via the ${}^3T_1(F)$ - ${}^1T_2(G)$ absorption.

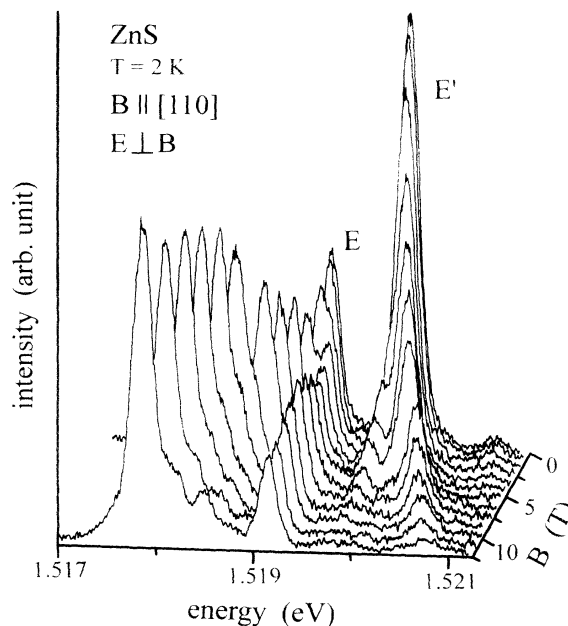


FIG. 6. The Zeeman behavior of the E, E' doublet of the $\text{Ni}^{2+}[{}^3T_1(P)$ - ${}^3T_1(F)]$ luminescence in cubic ZnS at $T = 2 \text{ K}$ observed in the Voigt configuration with the magnetic field aligned parallel to the $[110]$ axis and the polarization $E \perp B$.

ponents of the high-energy E' line decreases systematically whereas that of the components of the low-energy E line increases. This demonstrates that both emissions take place in the same center, but have different excited states. Obviously, the high-energy line has to be interpreted as a "hot" ZPL. The energy splitting of the E, E' doublet of $820 \pm 15 \mu\text{eV}$ corresponds well to the energy separation between the T_2 and the E state in the excited ${}^3T_1(P)$ multiplet derived from the Zeeman results shown in Fig. 3. Thus the E emission at 1.51923 eV and the hot E' emission at 1.5205 eV are attributed to the T_2 - T_1 and the E - T_1 transition, respectively. This interpretation is supported by luminescence spectra recorded under resonant excitation in the ZPL O showing only the low-energy E line of the E, E' doublet.¹⁹ Obviously, at $T = 2 \text{ K}$ no thermal equilibrium is reached in the ${}^3T_1(P)$ multiplet during its lifetime. This behavior is unusual for luminescent transition metal states, but explainable by the extraordinarily short lifetime of 100 ps established for the ${}^3T_1(P)$ state of Ni^{2+} in ZnS, recently.¹⁹ In general, thermal equilibrium is established by resonant one-phonon transitions between the close lying fine structure states. The probability of these transitions is basically proportional to the density of phonon modes and thus increases with increasing transition energy, at least for small splittings.³¹ In a magnetic field the increase of the energy splittings of the E, E' doublet of Ni^{2+} enhances the probability of one-phonon transitions from the higher Zeeman components. This explains the intensity development of the Zeeman components of the E, E' doublet shown in Fig. 6.

Figure 7 depicts the splittings of the E, E' doublet in a magnetic field applied parallel either to the $[110]$ axis or

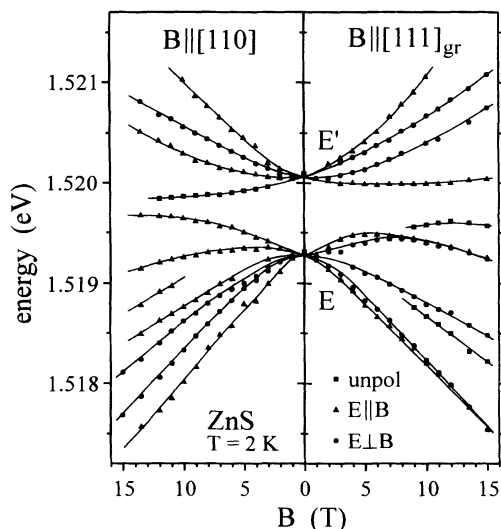


FIG. 7. The Zeeman splitting of the E, E' doublet of the $\text{Ni}^{2+} [{}^3T_1(P)-{}^3T_1(F)]$ luminescence in cubic ZnS at $T = 2$ K observed in the Voigt configuration with the magnetic field aligned parallel to the $[110]$ and the $[111]_{\text{gr}}$ axis, respectively.

to the $[111]_{\text{gr}}$ growth direction. A complex nonlinear behavior is observed, which is clearly different for the E and the E' line. The investigated sample as well as the sample orientations are the same as for the Zeeman investigation of the O absorption (Fig. 3). Consequently, the magnetic field dependence of the excited states is known and must be present in the Zeeman pattern of the E, E' doublet, (Fig. 7). Indeed, a detailed analysis taking into account the observed splittings in the ${}^3T_1(P)$ state shows that the energy shifts and polarizations of all observed components can be explained, assuming a threefold-degenerate T_1 ground state. The resulting splitting of the $T_1-{}^3T_1(F)$ state is given in Fig. 8. The two outer components shift linearly with the magnetic field, whereas the central component behaves nonlinearly at low fields and shifts parallel to the high-energy component at higher fields, indi-

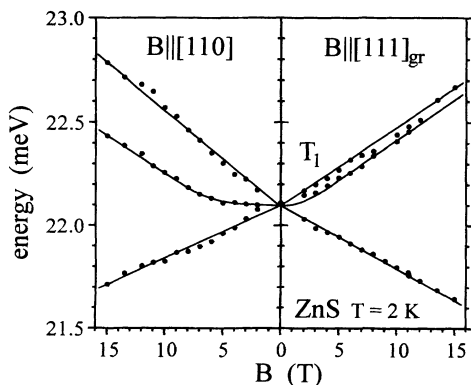


FIG. 8. The Zeeman splitting of the $T_1-{}^3T_1(F)$ state of Ni^{2+} in cubic ZnS at $T = 2$ K for the magnetic field oriented parallel to the $[110]$ and the $[111]_{\text{gr}}$ axis, respectively.

cating an additional vibronic state directly below the T_1 state.

IV. DISCUSSION

Ni^{2+} has an electronic d^8 configuration which splits into a variety of singular and triplet states due to the combined action of the electron-electron interaction and the tetrahedral crystal field (H^0).² Figure 9 depicts a rough term scheme showing only the ${}^3T_1(F)$ and the ${}^3T_1(P)$ states studied in the present paper. In both states the dominating fine structure interaction is the spin-orbit interaction resulting in an A_1, E and T_2, E term sequence in the ${}^3T_1(F)$ ground state and the reverse one in the ${}^3T_1(P)$ excited state, where the T_1 and the A_1 state are expected some 10 meV above the T_2, E doublet.² Thus the A_1 state observed 1830 μeV above the T_2 state cannot be explained in a static model. However, considering the electron-phonon interaction, an additional A_1 vibronic state originating at a one-phonon state is situated slightly above the E state^{5,24} as indicated in Fig. 9. The aim of the discussion is to evaluate the experimental results in view of the appropriate dynamical description. The most obvious changes caused by an additional C_{3V} crystal field (right-hand side of Fig. 9) are a trigonal splitting of the T_2 state into an A_1, E doublet and an alteration of the dipole selection rules. Instead of the unpolarized ZPL O , four polarized transitions can be observed for axial centers at zero magnetic field. The zero magnetic field transitions discussed in Sec. III for the perfectly cubic as well as the axial Ni^{2+} center in ZnS are indicated by arrows.

Neglecting the electron-phonon interaction, the Zeeman behavior of the T_2 and the E state can be calculated assuming a $J = 2$ state.^{11,32} Figure 10 compares

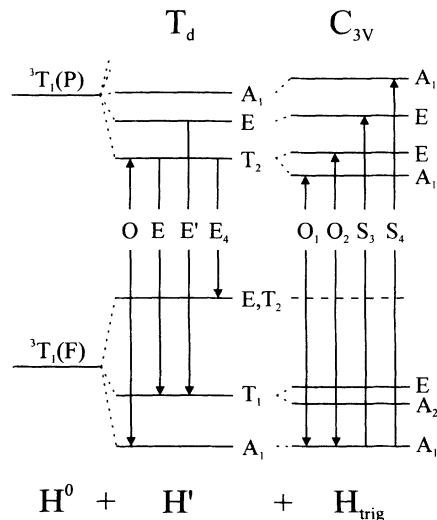


FIG. 9. Schematic term scheme of Ni^{2+} (d^8 configuration) in T_d and C_{3V} symmetry. H^0 includes the electron-electron interaction and the cubic crystal field, H' contains the spin-orbit interaction and a dynamical Jahn-Teller effect, and H_{trig} represents the trigonal crystal field. The zero field fine structure transitions observed in this work are indicated by arrows.

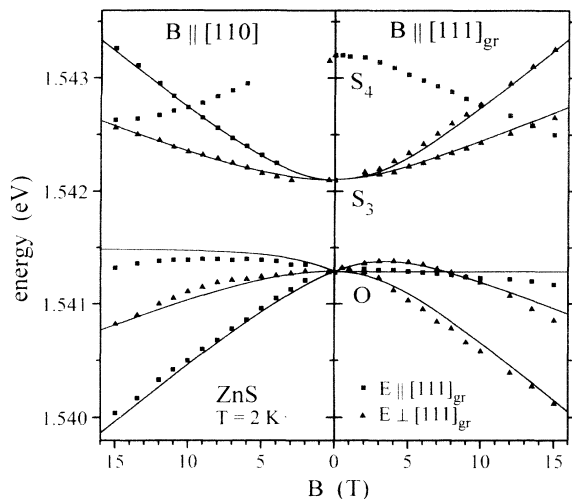


FIG. 10. The Zeeman behavior of the ZPL's of the ${}^3T_1(F)$ - ${}^3T_1(P)$ absorption of Ni^{2+} in cubic ZnS at $T = 2$ K for the magnetic field aligned parallel to the $[110]$ and the $[111]_{\text{gr}}$ axis, respectively. Points represent the experimental results and full lines give a fit using a static model. The parameters of the fit are given in the text.

the nonlinear Zeeman splittings observed for the cubic Ni^{2+} center with a theoretical fit assuming a $J = 2$ state and taking the second-order spin-orbit interaction into account. Good agreement between experiment and the fit is obtained, using a zero field splitting of the E, T_2 doublet of $820 \pm 20 \mu\text{eV}$ and an isotropic g factor of 0.91 ± 0.02 . However, despite the good qualitative agreement, the A_1 state and the g factor below 1 are not compatible with a static description. Additionally, at higher-magnetic fields the two high energy components of the O absorption are systematically shifted towards lower energies compared to the theoretical prediction. This behavior indicates term interactions with higher lying states, which are not expected in a static model. Furthermore, the S_4 transition is diamagnetic at low fields, but shifts towards lower energies at higher fields indicating the presence of further, nearby vibronic states. The observed term interactions as well as the presence of the A_1 state just above the E, T_2 doublet prove the vibronic origin of the states and thus call for a dynamical Jahn-Teller effect in the ${}^3T_1(P)$ state of Ni^{2+} .

The main problem of the Jahn-Teller calculations is the correct choice of phonon modes involved, since often different approaches can reproduce the observed fine structure. Considering a T_1 -type electronic state, in principle, E and T_2 modes have to be taken into account in T_d symmetry. For the ${}^3T_1(P)$ state of Ni^{2+} two different models considering a dynamical Jahn-Teller effect have been proposed.^{5,22} Both are able to explain a vibronic A_1 state close above the E, T_2 doublet. In a first attempt, based on a comparison of the fine structure observed in cubic and hexagonal ZnS samples, the simultaneous coupling to one E and one T_2 mode with energies of 8.7 meV has been proposed.⁵ The whole sideband except the first broad structure shifted by 6.3 meV has been attributed to

undisturbed host as well as local phonon replicas. However, our results indicate a vibronic character of the sideband. Recently, a different theoretical concept^{22,24} has been developed for the system CdS:Ni on the basis of exceptionally detailed experimental data.¹³ In this case the coupling to local T_2 modes is assumed to be dominant since only these modes depend on the mass of the central ion, which is a precondition to explain the observed isotope shifts. Taking into account one T_2 mode with an energy of 39 meV, not only the $O_{1,2}$ and $S_{1,2}$ but also the next "phonon" replicas can be attributed to vibronic states. Good agreement between experimental and theoretical line positions is established for a Huang-Rhys factor of 0.95. Additionally, the derived solution reproduces the observed Zeeman behavior and isotope splittings correctly without further free parameters. The local environment of Ni ions on cation sites in ZnS and CdS is similar. Thus it seems likely that in both systems Ni experiences a similar Jahn-Teller interaction. Indeed, comparing the ${}^3T_1(F)$ - ${}^3T_1(P)$ transitions of Ni^{2+} in ZnS and CdS, a good qualitative agreement of the fine structure, of the phonon sidebands, and of the isotope shifts (observed for axial centers¹³) can be stated. Additionally, the nonlinear Zeeman behavior in ZnS is found to be in excellent qualitative agreement with that calculated for CdS.²⁴ Especially the magnetic field dependence of the A_1 - ${}^3T_1(P)$ state, as well as its term interaction with the components of the T_2 state, is explained in the dynamical model. A quantitative comparison of the fine structure splittings shows that in CdS the E state lies at higher energy, which could be a hint for a stronger second-order spin-orbit interaction. Nevertheless, for quantitative statements, as well as a decision about the phonon modes involved in the electron-phonon interaction, detailed calculations are necessary. Thus ZnS:Ni is an ideal system to probe the reliability of the theoretical concept developed for CdS:Ni.

The fine structure of the ${}^3T_1(P)$ - ${}^3T_1(F)$ luminescence (Fig. 4) reflects the spin-orbit splitting of the ${}^3T_1(F)$ state.⁸ However, the magnitude of the splittings is smaller than expected from a static approach, indicating a dynamical Jahn-Teller effect in the ${}^3T_1(F)$ ground state too. A strong additional argument in favor of a dynamical description is given by the Zeeman behavior of the T_1 - ${}^3T_1(F)$ state (Fig. 8). The nonlinear magnetic field dependence of the central component of the T_1 state has to be attributed to a term interaction with a state lying directly below the T_1 state not explainable in a static model. We failed to resolve this state in zero magnetic field spectra, but the temperature dependence of the FWHM of the E emission enables us to locate this level. Figure 11 compares the FWHM's of the O absorption and the E emission revealing quite different behavior. The FWHM of the E emission starts to increase at lower temperatures and is larger than that of the O absorption at higher temperatures. The increase of the FWHM's with increasing temperature results from a reduction of the dephasing times of the involved states due to the interaction with thermally activated phonons. For the investigated multilevel system in the relevant temperature region, resonant absorption and emission of

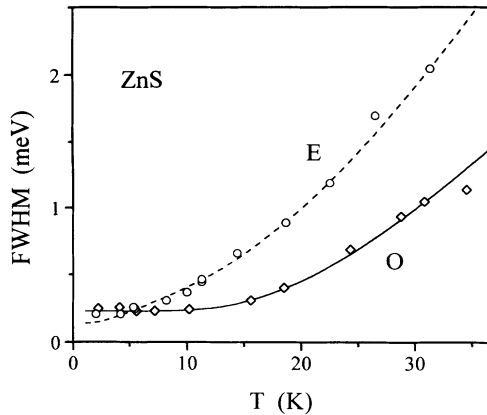


FIG. 11. The temperature dependence of the FWHM's of the *O* absorption and the *E* emission of the ${}^3T_1(F)$ - ${}^3T_1(P)$ transition of Ni²⁺ in cubic ZnS. Lines represent fits assuming resonant one-phonon transitions as dominating dephasing processes in the investigated temperature region.

phonons is the dominant dephasing process. The temperature dependence of the corresponding transition rate W is given by³¹

$$W(T) = W(0) \exp\left(\frac{\hbar\omega}{2kT}\right). \quad (3)$$

Here $W(0)$ is the spontaneous decay rate of the excited fine structure state. The FWHM of the *O* absorption can be fitted using a phonon frequency $\hbar\omega$ of 6.0 meV and a spontaneous transition rate $W(0)$ of 5.3 THz. The phonon energy corresponds well to the energy difference between the T_2 state and the vibronic state leading to the first broad phonon replica in absorption (Fig. 1). Thus the temperature dependence of the *O* transition is determined by dephasing processes in the excited ${}^3T_1(P)$ state and the contribution of the A_1 - ${}^3T_1(F)$ ground state can be neglected in the investigated temperature region. This is no longer the case for the *E* transition having the same excited but a different ground state. The additional dephasing of the T_1 - ${}^3T_1(F)$ ground state accounts for the larger FWHM of the *E* transition. A good fit of the FWHM of the *E* emission is obtained considering the resonant one-phonon transition in the excited ${}^3T_1(P)$ multiplet and an additional one-phonon process with a phonon energy $\hbar\omega$ of 0.63 meV and a spontaneous transition rate $W(0)$ of 0.21 THz. The second process takes place in the ${}^3T_1(F)$ ground state between the T_1 state and a second level 0.63 meV apart. In conjunction with the Zeeman results (Fig. 8), this level can be located below the T_1 state.

Static crystal field theory is not able to explain an electronic level directly below the T_1 level in the ${}^3T_1(F)$

ground state. However, quite similar experimental observations for CdS:Ni²⁺ could be explained within a dynamical model assuming the coupling to one T_2 mode.²⁴ A reasonable fit has been obtained using a gap T_2 mode with an energy of 21 meV and a Huang-Rhys factor of 0.97. Now a similar situation is expected for the system ZnS:Ni.

V. CONCLUSION

The fine structure of the ${}^3T_1(F)$ - ${}^3T_1(P)$ transition of isolated Ni²⁺ ions in cubic ZnS has been investigated by means of absorption and luminescence spectroscopy. Comparing the spectra of various intentionally as well as unintentionally Ni-doped samples and investigating the influence of magnetic fields as well as crystal temperature, the fine structure transitions of the perfectly cubic as well as of one axial Ni²⁺ center are determined. The axial center is connected with polymorphic lattice distortions. The Zeeman behavior of the Ni²⁺ transitions is found to be nonlinear due to pronounced term interactions. The intensity development of the Zeeman components proves hot luminescence from the excited *E* state, demonstrating that no thermal equilibrium is established during the lifetime of the ${}^3T_1(P)$ state. Additionally, a Fano resonance is identified in the sideband of the absorption and attributed to the coupling of a gap mode with a continuum of phonon modes.

The experimental results presented prove static models to be inadequate to describe the fine structure of the Ni²⁺ states demonstrating dynamical Jahn-Teller interactions. A detailed comparison of the fine structure of the Ni²⁺ multiplets in ZnS and in CdS demonstrates a far reaching equivalence, indicating similar fine structure interactions in both systems. Thus the theoretical concept²⁴ developed to describe the system CdS:Ni should be transferred to the case of ZnS:Ni. Both the fine structure of the ${}^3T_1(F)$ ground and the ${}^3T_1(P)$ excited state is determined by spin-orbit interaction and a dynamical Jahn-Teller coupling to local T_2 modes of the Ni center. It can be expected that the fine structure, as well as the magnetic field dependence, can be reproduced correctly, allowing us to evaluate the general validity of the theoretical concept.

In conclusion, the importance of the electron-phonon interaction for the fine structure and the Zeeman behavior of Ni²⁺ in cubic ZnS is demonstrated. Detailed experimental results are presented and qualitatively discussed. A quantitative explanation of the rich experimental data has to be given by detailed calculations, which are in progress.

ACKNOWLEDGMENT

The authors wish to thank Dr. R. Broser for supplying the crystals.

- ¹R. Papalardo and R.E. Dietz, *Phys. Rev.* **123**, 1188 (1961).
- ²H.A. Weakliem, *J. Chem. Phys.* **62**, 2117 (1962).
- ³M.L. Reynolds, W.E. Hangston, and G.F.J. Garlick, *J. Phys. C* **2**, 361 (1969).
- ⁴U.G. Kaufmann, P. Koidl, and O.F. Schirmer, *J. Phys. C* **6**, 310 (1973).
- ⁵U.G. Kaufmann and P. Koidl, *J. Phys. C* **7**, 791 (1974).
- ⁶G. Roussos and H.-J. Schulz, *Phys. Status Solidi B* **100**, 577 (1980).
- ⁷G. Roussos and H.-J. Schulz, *Solid State Commun.* **51**, 663 (1984).
- ⁸G. Goetz, G. Roussos, and H.-J. Schulz, *Solid State Commun.* **57**, 343 (1984).
- ⁹B. Mueller, G. Roussos, and H.-J. Schulz, *J. Cryst. Growth* **72**, 360 (1985).
- ¹⁰R. Heitz, A. Hoffmann, and I. Broser, *Phys. Rev. B* **48**, 8672 (1993).
- ¹¹R. Germer, F. Seliger, U. Kaufmann, and J. Schneider, *J. Phys. C* **14**, 2535 (1981).
- ¹²I. Broser, R. Broser, E. Birkicht, and A. Hoffmann, *J. Lumin.* **31/32**, 424 (1984).
- ¹³I. Broser, A. Hoffmann, R. Germer, R. Broser, and E. Birkicht, *Phys. Rev. B* **33**, 8196 (1986).
- ¹⁴D. Wasik, Z. Liro, and M. Baj, in *Proceedings of the 19th International Conference on Defects in Semiconductors, Warsaw, 1988*, edited by W. Zawadzki (Institute of Physics, Polish Academy of Science, Warsaw, 1988), p. 1197.
- ¹⁵D. Wasik, M. Baj, and Z. Liro, *Acta Phys. Pol. A* **79**, 319 (1991).
- ¹⁶A. Hoffmann, B. Lummer, Ch. Fricke, R. Heitz, and I. Broser, *J. Cryst. Growth* **117**, 640 (1992).
- ¹⁷L. Podlowski, R. Heitz, A. Hoffmann, and I. Broser, *J. Lumin.* **53**, 401 (1992).
- ¹⁸R. Heitz, A. Hoffmann, and I. Broser, *Opt. Mater.* **1**, 75 (1992).
- ¹⁹R. Heitz, L. Eckey, A. Hoffmann, and I. Broser, *Physica B* **185**, 234 (1993).
- ²⁰R. Heitz, P. Thurian, A. Hoffmann, and I. Broser, *Mater. Sci. Forum* **83-87**, 1247 (1992).
- ²¹I. Broser, R. Germer, and H.-J. Schulz, *Phys. Status Solidi B* **101**, 181 (1980).
- ²²B. Nestler, A. Hoffmann, L.B. Xu, U. Scherz, and I. Broser, *J. Phys. C* **20**, 4613 (1987).
- ²³U. Scherz, A. Hoffmann, B. Nestler, and L.B. Xu, *J. Lumin.* **40&41**, 411 (1988).
- ²⁴J. Schoepp, R. Heitz, A. Hoffmann, and U. Scherz, *Mater. Sci. Forum* **143-147**, 815 (1994).
- ²⁵R. Frerichs, *Naturwissenschaften* **33**, 281 (1946).
- ²⁶A. Hoffmann, R. Heitz, and I. Broser, *Phys. Rev. B* **41**, 5806 (1990).
- ²⁷P. Thurian, R. Heitz, T. Jentzsch, A. Hoffmann, and I. Broser, *Physica B* **185**, 239 (1993).
- ²⁸U. Fano, *Phys. Rev.* **124**, 1866 (1961).
- ²⁹J.M. Baranowski, J.M. Noras, and J.W. Allen, *J. Phys. C* **7**, 4529 (1974).
- ³⁰U. Pohl and H.-E. Gumlich, *Phys. Rev. B* **40**, 1194 (1989).
- ³¹B. Di Bartolo, *Optical Interactions in Solids* (Wiley, New York, 1968), p. 343.
- ³²P.J. Dean and R.A. Faulkner, *Phys. Rev.* **185**, 1064 (1969).
- ³³M. Skowronski and Z. Liro, *J. Lumin.* **24/25**, 253 (1981).